ADVANCED NAVIGATION STRATEGIES FOR AN ASTEROID SAMPLE RETURN MISSION

J. Bauman,* K. Getzandanner,† B. Williams,* K. Williams*

The proximity operations phases of a sample return mission to an asteroid have been analyzed using advanced navigation techniques derived from experience gained in planetary exploration. These techniques rely on tracking types such as Earth-based radio metric Doppler and ranging, spacecraft-based ranging, and optical navigation using images of landmarks on the asteroid surface. Navigation strategies for the orbital phases leading up to sample collection, the touch down for collecting the sample, and the post sample collection phase at the asteroid are included. Options for successfully executing the phases are studied using covariance analysis and Monte Carlo simulations of an example mission to the near Earth asteroid 4660 Nereus. Two landing options were studied including trajectories with either one or two burns from orbit to the surface. Additionally, a comparison of post-sample collection strategies is presented. These strategies include remaining in orbit about the asteroid or standing-off a given distance until departure to Earth.

INTRODUCTION

Flyby and rendezvous missions to asteroids have been accomplished using navigation techniques derived from experience gained in planetary exploration. The NEAR Shoemaker spacecraft was placed into orbit and soft-landed on the surface of the asteroid 433 Eros in February 2001, using a navigation strategy that relied on a combination of Deep Space Network (DSN) radiometric tracking and optical landmark tracking obtained from on board images. 1 Although it also carried a laser ranging instrument, the ranging data were used for asteroid shape model improvements and trajectory reconstruction, and thus it did not directly impact trajectory estimates used for propulsive maneuvers. In the final hours leading up to landing, the laser ranging data were downlinked for real-time monitoring of range to the surface in the direction the instruments were pointed and not necessarily to nadir (i.e., the slant range to the surface); however, the slant range information was not used to influence the landing sequence. In addition, NEAR Shoemaker did not include any navigation autonomy to change or abort the landing sequence once it had been initiated by ground command. Although the scenario was successfully used for landing NEAR Shoemaker, processing the additional slant range information with an appropriate level of on board autonomous navigation can reduce the mission risk for a sample return mission. On the other hand, the Hayabusa mission provides an example of proximity operations for an asteroid sample return using in situ ranging and a high level of onboard autonomous navigation; however, on board navigation issues were encountered that increased mission risk and reduced the certainty that a sample was obtained.2

^{*} KinetX, Inc. Space Navigation and Flight Dynamics Practice, 21 West Easy St. #108, Simi Valley, California 93065

[†] NASA Goddard Space Flight Center, Navigation & Mission Design Branch, Greenbelt, Maryland 20771

For the current analysis of navigation strategies, a notional reference mission was designed to return a sample from the near Earth asteroid 4660 Nereus. The example scenario includes establishing a stable near-circular orbit about 4660 Nereus prior to descending to land and collecting a sample. The orbit will remain passively stable requiring no station keeping for 7 days, at which time orbit maintenance will be needed to reduce the orbit eccentricity. For this example mission, the spacecraft perturbations are dominated by solar radiation pressure; however, this might not be the case for a more massive target body. When orbit maintenance is needed, the average correction maneuver will cost about 0.5 cm/sec of ΔV . The details of the final touchdown and sample collection technique are mission specific and are not covered here; however, the options for controlling the surface impact velocity are included. Prior to the orbit and touch down, the asteroid characteristics required for navigation (e.g., the gravity model, spin state, landmark locations, shape model, etc.) are determined during earlier phases of the rendezvous and survey orbits. The actual landing for sample collection is the result of a methodical refinement of asteroid spin state, shape and gravity models in addition to characterization and verification of the spacecraft dynamical models. Spacecraft dynamical models for solar radiation pressure, asteroid re-radiation effects and maneuver execution are included. The systematic study of navigation techniques to touch down on the asteroid surface for sample acquisition will compare (1) the effectiveness of a single de-orbit burn to the surface vs. a two-burn approach, (2) the usefulness of on board laser ranging to the surface vs. open-loop prediction (as used on NEAR-Shoemaker) for landing, and (3) an extended stay in orbit vs. a stand-off trajectory that stays in the neighborhood of the asteroid after the sample is acquired until the return maneuver to Earth.

PROBLEM STATEMENT

The proper balance between ground-based navigation and on board autonomous navigation is determined in this analysis by studying the evolution of the uncertainty in the relevant dynamic parameters. These parameters include the spacecraft position and velocity in an asteroid-centered, J2000 inertial frame and the asteroid spin state and gravity. The uncertainty in these parameters is relatively large early in the encounter and rendezvous phases, and is progressively lowered during survey and mapping phases until the landing and sample acquisition can be attempted. Autonomous navigation then processes the line-of-sight distance or slant range information and makes simple adjustments to the landing sequence, such as initiating a touchdown braking maneuver or a sequence abort, that are consistent with the uncertainties in the slant range and the pre-determined sequence. Practice landing attempts can be used to further reduce risk and test the actual level of precision that has been achieved for the dynamic models. Monte Carlo simulations are used to demonstrate these strategies for the realistic mission example.

Reference Mission Asteroid and Spacecraft Models

The reference mission target asteroid is based upon the near Earth asteroid (NEA) 4660 Nereus. For this analysis, the physical properties of the asteroid were estimated using available data on Nereus and similar asteroids (Table 1)³. The gravity harmonics for this study were selected arbitrarily to represent oblateness and equatorial ellipticity of the body so that representative spacecraft orbit perturbations would result. There are no known values for these parameters for 4660 Nereus. Selection of an actual asteroid as the basis of the reference target is done primarily for clarity in order to clearly display the methods and techniques that can be used as advanced navigation strategies. The outlined navigation strategy and resulting analysis, however, are not limited to this specific target asteroid and may be applicable to a diverse range of mission scenarios.

Table 1. Reference mission target asteroid physical properties

	Target Asteroid Proper	rties	
Mean Radius		0.165 km	
Density		1400 kg/m ³	
Mass		2.66 x 10 ¹⁰ kg	
GM		1.78 x 10 ⁻⁹ km ³ /s	
	Rt. Ascension (RA)	0°	
Spin State	Declination (DEC)	90°	
relative to J2000	Spin Rate	572.19 °/d	
J2 (Normalized)		0.01	
C22 (Normalized)		0.001	

Properties of the sample return spacecraft are presented in Table 2. The spacecraft is modeled as a spherical bus of fixed cross-sectional area with sun-fixed solar arrays for continuous sun tracking. The spacecraft mass in Table 2 is the total mass in orbit. It was chosen to represent a typical Discovery-class spacecraft.

Table 2. Reference mission spacecraft physical properties

Spacecraft Characteristics			
Mass	1005 kg		
SRP Area	13 m ²		
SRP Coeff.	1.1		

Reference Mission Design

An example mission design to 4660 Nereus was chosen with launch date of 01/30/2022 and an arrival date of 04/22/2023. The approach hyperbolic excess speed at Nereus rendezvous is 497 m/s. The rendezvous maneuver design and covariance analysis was carried out in a previous paper.⁴ In that paper, the scenario to rendezvous and establish a circular orbit at 500 m radius was analyzed, and then simulations were performed to determine estimates for the NEA's physical parameters and the uncertainties associated with them. For an actual mission, these steps would be performed before attempting to land and collect a sample.

The proximity operations navigation strategy for the representative mission is divided into the following segments: the asteroid rendezvous and approach phase, the survey phase, the stable orbit phase, the descent and sample collection phase, and the post sample collection orbit or stand-off phase. After rendezvous and during the approach and survey phase, initial estimates of model parameters for asteroid and spacecraft dynamics are obtained from the available tracking data. During the stable orbit leading up to the descent to touch down, the model parameters are continually refined and verified as part of the orbit determination process.

For the simulations at 4660 Nereus, an orbit of 500 m radius was chosen as the stable "home" orbit prior to descent. The spacecraft stays in this stable "home" orbit until the initiation of the landing approach, and will also return to this orbit if at any time the landing approach has to be aborted. The circular orbit period for the assumed asteroid physical parameters at this radius is 14.6 hours, and the orbital velocity is 5.9 cm/s. This stable orbit allowed seven days of tracking to be simulated without requiring any orbit correction maneuvers that would degrade the precision of the orbit estimate. At the end of seven days the orbit eccentricity had evolved from a value of 0.001 to 0.333 due largely to solar radiation pressure, and the orbital velocities at apoapsis and periapsis in the final perturbed orbit were 4.2 cm/s and 8.5 cm/s, respectively.

Figure 1 shows the orbit evolution over the seven-day arc around 4660 Nereus. The tick marks in Figure 1 are at one-hour intervals.

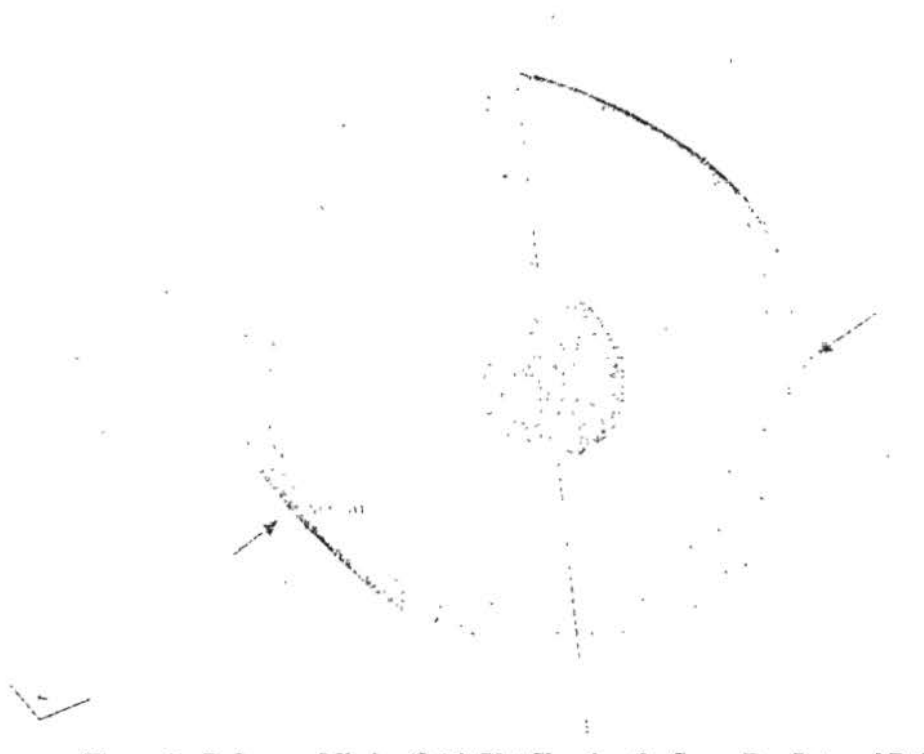


Figure 1. Reference Mission Orbit Plot Showing the Seven Day Interval Before Descent Beginning with a 5-degree Inclination from Nereus' Terminator Plane.

ORBIT COVARIANCE ANALYSIS

Covariance analysis was performed over a seven day arc of tracking data in the 500 m radius orbit shown in Figure 1 leading up to the orbit departure maneuver that sets up the descent to touch down for both the one-burn and two-burn scenarios described later. Tracking data were simulated over the seven days and consisted of one 8 hr track per day increasing to continuous tracking during the landing scenarios. The filter assumptions used in this analysis are shown in Table 3 and the tracking data weights assumed are shown in Table 4. The filter parameters were based on NASA's NEAR mission experience. ¹

Table 3. Orbit Phase Covariance Analysis Assumptions

Baseline Covari	ance Analysis Assumptions		
Estimated Parameters	A-priori Uncertainty (1σ)		
Spacecraft Initial State	50 km, 30 m/s		
Solar pressure	Effective cross section 5 m ² , 1σ Momentum transfer coefficient 1.5 (±10%)		
Stochastic acceleration	1.0 x 10 ⁻¹² km/s constant bias, 1σ 7.5 x 10 ⁻¹¹ km/s variable, 1σ 10 day time constant, 2 day batch size		
Maneuver Execution Errors	2% (magnitude and pointing) + 1 mm/s (magnitude), all 3σ		
Planetary and Asteroid Ephemerides	DE418 with correlated covariances and Nereus diagonal sigmas provided by JPL's Solar System Dynamics group		
Conside	er Parameters		
Station locations	Correlated covariance determined from VLBI processing		
UT1 and polar motion	0.34 msec, 15 nrad.		
Troposphere (wet and dry)	4 cm, 1 cm		
Ionosphere	5.0 x 10 ¹⁶ elec/m ²		

Table 4. Tracking Data Weights for Covariance Analysis

Data Type Data Weight	
2-Way Doppler	0.1 mm/s
2-Way Range	50 m
OpNav	1 pixel (25 µrad)

The resulting spacecraft Carteasian position and velocity covariance at the end of the seven-day tracking arc is shown in an upper-triangular format in Table 5. The off-diagonal covariance elements for the lower half of the symmetric matrix are not shown for clarity. The resulting one-sigma variance for position is about 70 cm and for velocity about 0.05 mm/s, immediately before the first burn in the landing approach sequence. This covariance was sampled to generate perturbations to the nominal state for the Monte Carlo analysis in the next section.

Table 5. Spacecraft State Covariance at End of Seven-Day Tracking Data Arc in J2000 Asteroid Centered Carteasian Coordinates. Units are meters for position and meters per second for velocity.

X	Y	Z	VX	VY	VZ
0.060	-0.111	-0.147	-1.59E-06	1.24E-05	-4.35E-06
	0.237	0.320	2.61E-06	-2.69E-05	9.37E-06
		0.451	3.38E-06	-3.75E-05	1.37E-05
			5.50E-11	-2.81E-10	9.80E-11
			1	3.14E-09	-1.13E-09
					4.37E-10

LANDING APPROACH STUDY

The goal of the landing approach study is to determine the effectiveness of a single de-orbit burn to the surface vs. a two-burn approach. The largest contributors to determining the effectiveness of each landing scenario are the ΔV required and the landing accuracy on the surface of Nereus. Two simulations were performed, one with a single burn and another with two burns, to deliver the spacecraft from identical orbit initial conditions to the same body-fixed latitude on the surface. The longitude was also fixed, but in a space-fixed coordinate frame, so landing time differences resulted in different body-fixed longitudes at the landing site. Each of these scenarios were simulated in a Monte Carlo study that integrated 1000 sample trajectories from immediately before the orbit descent maneuver to contact with the surface. The initial conditions were perturbed from the nominal by performing random draws on the corresponding initial condition covariance matrix for position and velocity that was generated from the orbit covariance analysis. The single and two burn scenarios both used the same initial condition covariance matrix. The maneuvers were perturbed from their nominal values by performing random draws from assumed spherical uncertainties of 2.33×10^{-2} mm/s (1- σ).

The actual orbit operations and descent maneuvers in the period leading up to the touch down event would rely on quick turn-around OpNav images for late updates to maintain precision of the trajectory prediction and the resulting touch down error ellipse on the surface. The rehearsals would include initial trial runs to a "checkpoint" on approach to the touchdown site, followed by return to orbit. The rehearsals allow verification of the precision of the touch down sequence in a step-by-step process before committing to the touch down itself. The final approach to landing is designed so that the spacecraft will continue safely in a low pass over the surface if the final burn is not executed. The same late update process used many times during the rendezvous and survey phases will also be used for updating the maneuvers leading up to touch down.

One-burn Descent Scenario

The simulated trajectory for the one-burn descent scenario is shown in Figure 2. For visual purposes the figure is drawn to scale with an arbitrary shape model scaled to represent the assumed radius of asteroid 4660 Nereus. The line drawn through the shape indicates the trajectory of the asteroid. The trajectory of the spacecraft is shown from apoapsis on 30-APR-2023 01:25:19.29 UTC through periapsis at 30-APR-2023 08:47:18.24 UTC. The maneuver occurs at 30-APR-2023 10:50:00.0 UTC. The single maneuver is used to target a specific latitude on the surface of Nereus. Note the abrupt change in direction of the orbit at the time of the burn is typical of orbital maneuvering about small bodies, even though the ΔV magnitudes are typically less than a few centimeters per second.



Figure 2. Simulated orbit for one-burn descent orbit. Tic marks denote 6 minute time intervals from apoapsis to touch down. Touch down time is displayed in figure.

Monte Carlo results are shown in Tables 5, 6, and 7 and Figure 3. Uncertainty levels for the results are shown for one standard deviation, 90^{th} percentile, 95^{th} percentile, and 99^{th} percentile. Table 5 shows the landing ellipse semi-major (a) and semi-minor (b) axes, and includes the orientation angle of the major axis of the ellipse relative to Nereus equator. Table 7 shows the statistics on the landing time for each level of uncertainty. Figure 3 shows a plot of the landing uncertainty ellipses for the various uncertainty levels for the one-burn descent scenario. Note that the landing error ellipse has an elongated shape with the largest dispersion in the approach velocity (down track) direction, and a much smaller dispersion normal to the approach velocity (cross track) direction. The overall dimensions of the landing uncertainty ellipse are 18.46 m by $2.10 \text{ m} (1-\sigma)$. Table 8 shows the statistics on the resulting vertical velocity at the surface, which is $6.98 \pm 0.24 \text{ cm/s} (1-\sigma)$.

Table 6. Monte Carlo Landing Ellipses for One-Burn Descent

Level	a [m]	b [m]	40.90 40.90	
1-Sig	9.23	1.05		
90%	18.90	2.15		
95%	21.68	2.47	40.90	
99%	25.55	2.91	40.9	

Table 7. Monte Carlo Landing Time Uncertainty for One-Burn Descent

Level	Δt [s]
1-Sig	31.39
90%	50.86
95%	61.07
99%	80.27

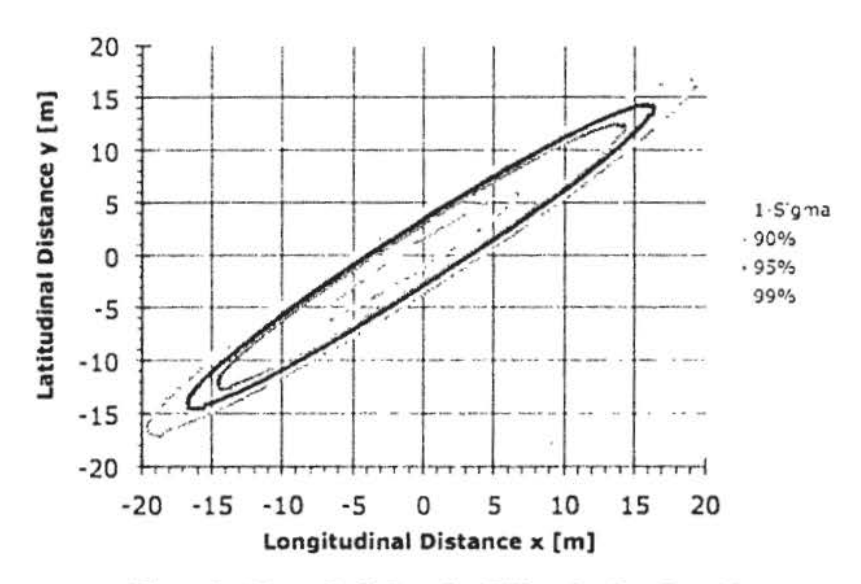


Figure 3. Monte Carlo Landing Ellipse for One-Burn Descent

Table 8. Monte Carlo Velocity Uncertainty at Surface for One-Burn Descent

	Vertical Velocity (cm/sec)	Horizontal Velocity (cm/sec)
Mean	11.2824	12.5606
1-Sig	0.1734	0.2522
90%	0.2852	0.4149
95%	0.3398	0.4943
99%	0.4466	0.6497

Two-burn Descent Scenario

The simulated trajectory for the two-burn descent scenario is shown in Figure 4. The figure is drawn to scale with an arbitrary shape model scaled to represent asteroid 4660 Nereus. The line drawn through the shape indicates the trajectory of the asteroid. The trajectory of the spacecraft is shown from apoapsis on 30-APR-2023 01:25:19.29 UTC through the first maneuver at 30-APR-2023 08:47:18.24 UTC. The second maneuver takes place at 30-APR-2023 11:08:13.92 UTC. The first maneuver is used to lower the spacecraft orbit radius to 50 meters. The second maneuver is used to target and land on a specific latitude on the surface of Nereus, identical to the latitude used in the one-burn descent scenario.

Monte Carlo results are shown for the two-burn descent scenario similarly to the results shown above for the one-burn case. Table 9 shows the landing ellipse semi-major (a) and semi-minor (b) axes, including the orientation angle of the major axis of the ellipse relative to Nereus equator. Table 10 shows the statistics on the landing time for each level of uncertainty. Figure 5 shows a plot of the landing uncertainty ellipses for the various uncertainty levels for the two-burn descent scenario. Note that the landing error ellipse for the two-burn case looks similar to the result for the one-burn case, but now the overall dimensions of the landing uncertainty ellipse are 12.60 m

by 0.52 m (1- σ). Table 8 shows the statistics on the resulting vertical velocity at the surface, which is 11.28 ± 0.17 cm/s (1- σ).

30-APR-2023 11:15:13 8778 UTC

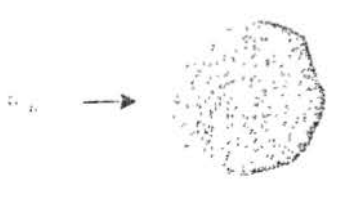


Figure 4. Simulated orbit for two-burn descent orbit. Tic marks denote 6 minute time intervals from apoapsis to touch down. Touch down time is displayed in figure.

Table 9. Monte Carlo Landing Ellipses for Two-Burn Descent

Level	a [m]	b [m]	Orient [deg] 36.6	
1-Sig	6.30	0.26		
90%	13.24 0.55	0.55	36.6	
95%	15.19	0.63	36.6	
99%	17.81	0.74	36.6	

Table 10. Monte Carlo Landing Time Uncertainty for Two-Burn Descent

Level	Δt [s]
1-Sig	21.63
90%	36.57
95%	40.75
99%	49.69

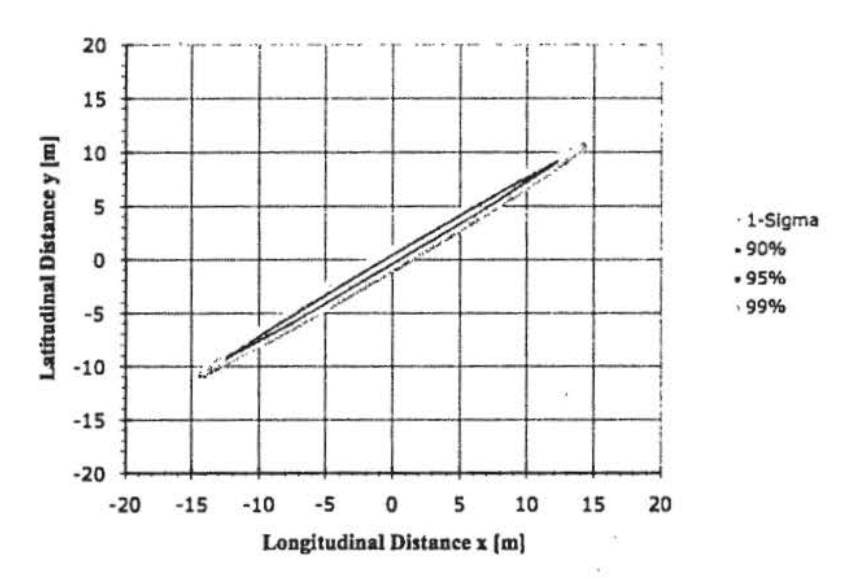


Figure 5. Monte Carlo Landing Ellipse for Two-Burn Descent

Table 11. Monte Carlo Velocity Uncertainty at Surface for Two-Burn Descent

	Vertical Velocity (cm/sec)	Horizontal Velocity (cm/sec)
Mean	6.9823	13.9547
1-Sig	0.2401	0.2818
90% +/-	0.3950	0.4635
95% +/-	0.4707	0.5522
99% +/-	0.6186	0.7258

The results of the Monte Carlo simulations show that both burns produce an elongated ellipse over the 1000 samples taken for each scenario. The major axes of both ellipses are in the direction of Nereus' rotation causing the ellipse to be stretched larger in that direction. However, the two-burn scenario produces a slightly smaller ellipse. This is due in part to the angle of impact being more normal to the surface for the two-burn case (39°) than that for the one-burn scenario (29°). This angle of impact also causes less uncertainty in the timing of the landing. The vertical impact velocities for both simulations stay within the 10 centimeter per second range, with the one-burn scenario having roughly half the value of the two-burn scenario due to its lower angle of impact. The impact of the spacecraft would normally be monitored in real time in order to perform one final burn right before impact in order to soften the landing to perhaps one or two cm/s. The simulations of these final burns are not with in the scope of this paper.

POST SAMPLE COLLECTION STUDY

After the sample is collected, there will typically be additional time until the optimal time to depart the asteroid for the return journey to Earth occurs. In some cases, this period may extend for weeks or months until the departure burn is required. The following simulations compare an extended stay in orbit to a standoff trajectory that stays in the neighborhood of the asteroid after the sample is acquired until the return maneuver to Earth is scheduled to occur. Both the orbit scenario and the standoff scenario were simulated by numerical integration of the trajectories with the full dynamic spacecraft and asteroid models given in Table 1 and Table 2.

Post Sample Collection Orbit Study

One option for staying in the vicinity of the asteroid after sample collection is to maintain an orbit about the body until the time of the departure for return to Earth. For this analysis, an orbit that is ideally circular at 500 m radius and 5-degrees inclined from the terminator plane was chosen as a "home" orbit because it is close enough to remain captured yet not so close that perturbations that change eccentricity result in close flybys of the surface. Maintenance maneuvers were performed to stay in a region close to the ideal home orbit. In this case, the orbit eccentricity grows with time due to gravitational and solar radiation pressure forces, so an eccentricity of 0.3 was arbitrarily chosen as the maximum allowed before performing propulsive maneuvers to re-circularize. When using these constraints, maneuvers were required about every 7 to 10 days, and the average ΔV usage over a 30-day interval was 0.041 m/s. For more massive asteroids, higher orbits would remain securely captured and maintenance maneuvers would not be as frequent nor fuel costs as high as they are for Nereus.

Post Sample Collection Stand-Off Study

The alternative to maintaining an orbit about an asteroid while waiting for the maneuver to begin the return trajectory to Earth is to place the spacecraft in a heliocentric orbit some distance from the body while maintaining a safe separation distance. This "standoff" trajectory should stay in the vicinity of the asteroid until the time of the departure maneuver in order to stay close to the optimal return trajectory to Earth and minimize the fuel required for the return. Occasional station keeping maneuvers are required to maintain separation from Nereus due to perturbations from Nereus gravitational attraction and solar radiation pressure. The maneuver delta-V requirements for example stand-off distances of 50 km to 200 km from Nereus are shown in Table 12.

Table 12. Delta-V Requirements for Stand-Off Trajectories At Nereus

Ir	Initial Conditions			Final Conditions after			'S
Radius (km)	Radii	Latitude (deg)	Radius (km)		Altitude (km)	Marie Contraction of the Contraction of	ΔV Required (m/s)/30d
50.00	303.03	90.00	68.08	412.63	67.92	-29.92	0.060
100.00	606.06	90.00	62.26	377.33	62.10	15.90	0.009
165.00	1000.00	90.00	100.48	608.95	100.31	53.70	0.016
200.00	1212,12	90.00	129.53	785.04	129.37	62.80	0.016

The ΔV required for the standoff trajectories was calculated based on the trajectories of each sample in order to keep the spacecraft within $\pm 30\%$ of the original offset radius from Nereus. Thirty percent was chosen to match the similar requirement to maintain an orbit eccentricity of less than or equal to 0.3 for the orbiting case. The maneuvers required in the standoff study occurred at different intervals, with the lowest stand-off of 50 km being the shortest at one maneuver every 14 days while the altitudes higher than 100 km occurred at about 25 to 28 day intervals. The maneuver ΔV for each case was normalized to an equivalent ΔV with a thirty-day interval for comparison to the orbit case above. Note that the ΔV for standoff radii greater than 100 km is less than half the fuel required for a similar orbit maintenance strategy in the "home" orbit with 500 m radius. It's also important to notice that the lowest ΔV value occurs at a radius of 100 km. Though the reason isn't clear, the most likely cause could be, as the spacecraft moves further away, Nereus gravitational influence drops sharply until it has practically no affect at all. Meaning, the main source of perturbation is solar radiation pressure. This also explains why in Table 12 the values of ΔV for the 165 and 200 km stand-off radii are the same.

CONCLUSIONS'

The comparison of the single burn descent to landing with the two burn scenario shows the benefits of the two burn scenario with a smaller landing error ellipse, although at the expense of about doubling the mean vertical landing velocity. However, in both scenarios the landing vertical speed is less than ~ 12 cm/s $(1-\sigma)$, which can easily be countered by a small maneuver near the surface that is activated by an on board range detector such as a laser ranger or low-power radar altimeter. The Monte Carlo results shown include the statistics on the time of landing, which are $31 \text{ s} (1-\sigma)$ and $22 \text{ s} (1-\sigma)$ for the one-burn and two-burn cases, respectively.

After collecting a sample, the issue of staying in orbit or standing off some distance from Nereus in a near-by heliocentric orbit until time to depart for the return to Earth was also analyzed. Maintaining the 500 m radius orbit about Nereus required maneuvers about every 7 to 10 days to keep the orbit eccentricity less than 0.3. These maneuvers required about 0.041 m/s of ΔV every 30 days. For the standoff trajectories beyond ~100 km from Nereus, the trajectory maintenance to remain with $\pm 30\%$ of the chosen separation distance occurred about every 25 to 28 days and used about 0.016 m/s of ΔV every 30 days. Hence, for Nereus the standoff trajectories are more appealing than remaining in orbit from both an operational and a ΔV standpoint. However, this may not be the case for larger asteroids since ΔV costs are then small for remaining in a stable orbit. I

REFERENCES

Williams, B. G., et al, "Navigation for NEAR Shoemaker: the First Spacecraft to Orbit an Asteroid," AAS/AIAA Astrodynamics Specialist Conference, Quebec City, Quebec, Canada, July 30-August 2, 2001, Paper AAS 01-371.

² Hayabusa reference

³ JPL Horizons web site, "http://ssd.jpl.nasa.gov/?horizons"

⁴ Getzandanner, K., et al, "Advanced Navigation Strategies for Asteroid Sample Return Missions," AAS George Born Symosium, Boulder, Colorado, May 13-14, 2010.